

# CONTINUOUS SCPT SIGNAL ENHANCEMENT BY IDENTIFYING, QUANTIFYING AND EXTRACTING FREQUENCY ANOMALIES WITHIN STATISTICALLY DESCRIBABLE BACKGROUND NOISE

Erick Baziw

Baziw Consulting Engineers Ltd., Vancouver, Canada

Gerald Verbeek

Baziw Consulting Engineers Ltd., Vancouver, Canada

Keywords: Continuous seismic CPT, real-time event detection, Kalman filter, Hidden Markov models

**ABSTRACT:** Among *in-situ* engineers there is considerable interest in the development of continuous seismic cone penetration test (C-SCPT). Until now the seismic measurements are generally done during pauses in the penetration of the CPT cone. Also to avoid that waves generated by the shear wave source would travel through the CPT rods to the receivers, the string is unclamped. Together they form a major interruption of the CPT process and extend the time to complete a CPT sounding substantially. The C-SCPT will make SCPT much more efficient and therefore easier to perform. At the same time it will substantially increase the requirements on the data acquisition system as data stacking (by repeating the seismic test several times at each depth) or performing the test from both the left and the right side of the probe is no longer possible. The most important consideration in C-SCPT is obviously the real-time signal enhancement and event detection. Baziw Consulting Engineer's (BCE) main focus in C-SCPT is in the design of sophisticated digital filters to increase the S/N. As part of this BCE implements a novel and robust model of the source wave: the Amplitude Modulated Sinusoid (AMS), which has shown to be a highly robust and accurate approximation for many analytical representations of seismic source waves (such as the exponentially decaying cyclic waveform, the mixed-phase Berlage wave, the zero-phase Ricker wave, and the zero-phase Klauder wave). In addition, the AMS wave has proven very accurate in modeling seismic data acquired during downhole seismic testing and passive seismic monitoring. The algorithm we developed for this application, the so-called *C-SCPT SEED*<sup>TM</sup> (Signal Enhancement and Event Detection) algorithm, uses real time Bayesian Recursive Estimation (BRE) digital filtering techniques to analyze the raw data. In this paper we will discuss this algorithm and provide practical examples to demonstrate that BCE's *C-SCPT SEED*<sup>TM</sup> algorithm provides considerable SCPT signal enhancement and event detection advantages when processing C-SCPT seismic data, such as: • Ability to identify source wave "events" embedded in high variance and correlated noise environments • Significant S/N improvement • Source wave arrival time estimation • Ability to derive noise statistics • Dominant frequency estimation.

## 1 INTRODUCTION

There is considerable interest in methods of geotechnical *in-situ* engineering that provide accurate estimates of the low strain ( $<10^{-4}\%$ ) *in-situ* shear and compression wave velocities ( $V_S$  and  $V_P$  respectively) and the associated absorption values ( $\alpha_S$  and  $\alpha_P$  respectively) in the ground, since these parameters form the core of mathematical theorems to describe the elasticity/plasticity of soils and they are used to predict the soil response (settlement, liquefaction or failure) to imposed loads (whether from foundations, heavy equipment, earthquakes or explosions (Andrus et. al. (1999) and Finn (1984)). Moreover, accuracy in the estimation of shear and compression waves velocities is of paramount importance, because these values are squared during the calculation of various geotechnical parameters such as the Shear Modulus (G), Poisson's Ratio ( $\mu$ ) and Young's Modulus (E).

Applied seismology techniques such as the seismic cone penetration test (SCPT) have gained extensive popularity in recent years since they allow for

the *in-situ* estimation of the low strain shear and compression wave velocities and the associated absorption values. The SCPT is a downhole seismic testing technique which was devised to measure seismic velocities directly through data obtained by installed seismic sensors in the cone penetrometer, in addition to the standard bearing pressure, sleeve friction and pore pressure sensors (Campanella et al. 1986). The seismic cone (SC) has proven to be a very accurate and reliable tool in the determination of  $V_S$  and  $V_P$  profiles. The advantages of the seismic cone consist of excellent soil probe coupling, a controllable source and cost effectiveness because it is a retrievable probe. Details of the seismic cone, the downhole test procedures, and comparisons with the crosshole results at several sites have been described by Campanella et al (1986).

In general terms, the cone is advanced to the depth of interest using a hydraulic reactionary pushing. The advance is halted at one meter (or other such increment) intervals. When the cone is at rest, a seismic event is caused at the surface using a hammer blow or explosive charge, causing seismic waves to propagate from the surface through the soil

to be detected by seismic sensors installed in the cone penetrometer. This event is recorded and the penetrometer is advanced another increment and the process is repeated. Interval velocities are calculated over the depth increment under study (Campanella et al. 1989; Baziw 1993 and 2002 ) from the estimated seismic wave arrival and/or relative arrival times.

In the standard SCPT techniques implemented the in-situ  $V_s$  and  $V_p$  interval velocities are determined by firstly obtaining the corresponding time series relative arrival times as the probe is advanced into the soil profile. The relative arrival times can be obtained by utilizing the reverse polarity or cross-correlation techniques (Campanella et al. (1986) and Baziw (1993 and 2002a)). The SCPT is a relatively time consuming process compared to the CPT in that pauses in the penetration of the CPT cone are required and the string is required to be unclamped so that waves generated by the shear wave source do not travel through the CPT rods to the receivers. In addition, data stacking is required so that the signal-to-noise ratio (SNR) is increased. Data stacking in SCPT involves generating multiple sources and averaging the recorded seismic data so that random noises are minimized.

The development of a continuous SCPT (C-SCPT) has been gaining considerable interest among *in-situ* engineers so that the issue of SCPT latency can be addressed. In the C-SCPT configuration seismic source waves are generated as the penetrometer is pushed into the ground without stopping to unclamp the string, turning the rig/truck engine off, data stacking, and generating sources on both the left and the right side of the probe for the case of SH wave interval velocity investigations. This of course offers a real challenge in terms of seismic signal processing as the SNR of the recorded C-SCPT seismic data will be considerably lower compared to standard SCPT data. Furthermore, an event detection and arrival time estimation capability in C-SCPT is desired where first approximation interval velocity are calculated as the probe is pushed into the ground. BCE has been developing new techniques to address the challenges presented by C-SCPT. A particularly promising algorithms is the so called the so-called *C-SCPT SEED*<sup>TM</sup> (Signal Enhancement and Event Detection) algorithm.

## 2 C-SCPT SIGNAL ENHANCEMENT AND EVENT DETECTION

Standard SCPT signal processing algorithms typically rely upon off-line analysis techniques such as applying zero phase digital frequency filters to the raw time series data to separate the measurement noise from the desired source waves (Baziw (1993 and 2002a)). This is generally feasible due to the

fact that there is typically significant frequency spectra separation between the source waves and measurement noise (when source wave reflections are not present). Subsequent to the application of the zero phase digital frequency filters polarization analysis is applied so that the filtered responses on the x, y, and z components (for a triaxial configuration) are rotated onto a single full waveform (Baziw (2004a and 2004b)).

The C-SCPT signal processing requirements are considerably more challenging due to the fact that seismic data is recorded in a significantly higher noise environment, there is not a distinct separation between the frequency and associated phase components of the source waves and measurements noise, data stacking cannot be carried out and the real-time nature of the C-SCPT.

Due to the real-time nature of the C-SCPT and the overlap of the source wave and measurement noise frequency spectra, sophisticated real-time recursive Bayesian estimation techniques are applied to address the signal enhancement of the C-SCPT acquired time series. As previously stated, the algorithm utilized for C-SCPT signal processing and event detection is referred to as *C-SCPT SEED*<sup>TM</sup>. A fundamental component of the *C-SCPT SEED*<sup>TM</sup> is modeling of the source wave as an amplitude modulated sinusoid (AMS).

### 2.1 Amplitude Modulated Sinusoid (AMS)

The AMS has been demonstrated to be a highly robust and accurate approximation for many analytical representations of seismic source waves such as the exponentially decaying cyclic waveform, the mixed-phase Berlage wave, the zero-phase Ricker wave, and the zero-phase Klauder wave (Baziw (2002b, 2004b, 2005, 2006, 2007, and 2011)). In addition, the AMS wave has proven very accurate in modeling seismic data acquired during downhole seismic testing and passive seismic monitoring.

The mathematical representation of the AMS source wave is given as

$$x_1(t) = x_2(t) \sin[\omega t + \varphi] \quad (1)$$

where  $x_1(t)$  is an approximation to the seismic source wave,  $x_2(t)$  is the seismic wave's amplitude modulating term (AMT),  $\omega$  is the dominant frequency of the wave, and  $\varphi$  is the corresponding phase.

Baziw and Ulrych (2006) demonstrate the robustness of the AMS model by considering the zero phase Ricker wave. Although, the Ricker wave has a peak frequency, it doesn't have a specific sinusoidal term and as was shown by Baziw and Ulrych (2006) the AMS model was able to reconstruct the desired wave by applying an appropriate amplitude modulating term.

Amini and Howie (2005) utilized a finite difference program (FLAC) to model downhole seismic source waves. Figure 1 illustrates the simulated source wave generated by Amini and Howie obtained by personal communication. The source wave shown in Fig. 1 was generated by assuming a uniform halfspace with an in-situ shear wave velocity of 180 m/s and a sampling interval of 0.02 ms. Superimposed upon the finite difference source wave is a scaled 140 Hz sinusoid with zero crossing at 10.3 ms. Also superimposed upon the source wave illustrated in Fig. 1 is an exponential decay peaking at 15 ms and decaying at an exponential rate of 0.8/ms.

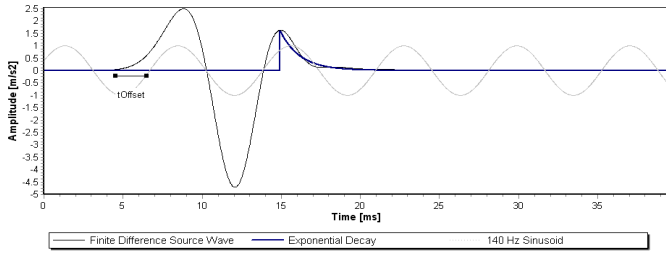


Figure 1. Finite difference source wave with superimposed 140 Hz sinusoid and exponential decay with rate 0.8/ms.

AMS real data examples are provided from downhole seismic data captured during a SCPT. The SCPT real data examples were captured with high precision and high bandwidth (1 Hz to 10 KHz) piezoelectric accelerometers which have an operational amplifier integrated within the sensor. The piezoelectric accelerometers have highly desirable rise and decay times of approximately 5  $\mu$ s. These fast rise and decay times result in recorded traces where the input of acoustic waves and ambient noise are recorded with minimal or no sensor distortion.

Figure 2 illustrates noisy SCPT data recorded at a depth of 15 m. The high noise energy is due to high frequency rod noise traveling down the steel extension rods and due to the close radial proximity of the source (Baziw (1993) and Baziw et. al. (2000)). Figure 3 illustrates the seismic data shown in Fig. 2 superimposed upon the same seismic trace filtered with a zero phase shift 8<sup>th</sup> order Butterworth 10 Hz to 150 Hz bandpass filter applied. Also superimposed upon the filtered seismic trace is a 73 Hz sinusoid. As is evident from Fig.3, the real SCPT source wave can be modeled as amplitude modulated sinusoid.

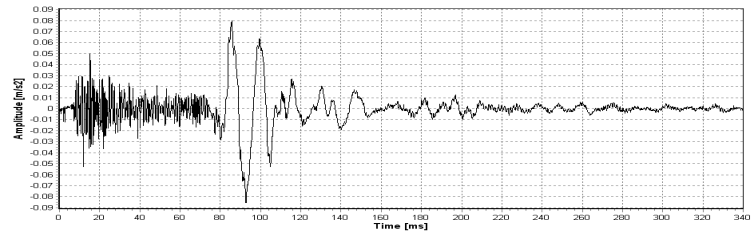


Figure 2. AMS real data example recorded during a SCPT.

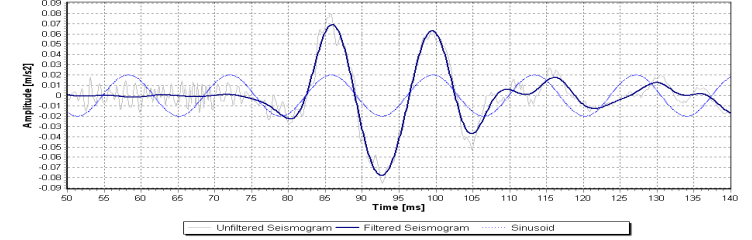


Figure 3. Seismic trace in Fig. 3 filtered with a 10Hz to 150Hz frequency filtered applied and a 73Hz sinusoid superimposed.

## 2.2 Gauss-Markov Measurement Noise Model

To facilitate greater source wave and measurement noise characterization the measurement noise is modeled as a Gauss-Markov process as opposed to simply being defined by a band of frequencies. By analyzing the autocorrelation and power spectrum of a large number of SCPT measurement noise time series it was possible to identify a mathematical model which sufficiently fits the SCPT measurement noise process. Figure 4 illustrates the autocorrelation function and power spectral density of common random processes (Gelb (1974)). A Gauss-Markov process can be used to describe many physical phenomena (Baziw (2002)) and is a good candidate to model the SCPT background noise.

The Gauss-Markov process has a relatively simple mathematical description. As in the case of all stationary Gaussian processes, specification of the process autocorrelation completely defines the process. The variance,  $\sigma^2$ , and time constant,  $T_c$  (ie.,  $\beta = 1/T_c$ ), define the first-order Gauss-Markov process. These parameters are derived from the seismic time series by windowing on the noise portion of the trace and calculating the autocorrelation of the ambient noises (Baziw (2002b and 2005)). The discrete mathematical equation for a Gauss-Markov process is given as

$$\begin{aligned} n_{k+1} &= a_w n_k + b_w w_k \\ a_w &= e^{-\beta\Delta} \text{ and } b_w = \sqrt{1 - e^{-2\beta\Delta}} \end{aligned} \quad (2)$$

In eq. (2),  $\Delta$  is the sampling rate and  $w_k$  is a zero-mean, timewise-uncorrelated, unit-variance sequence with a Gaussian probability distribution function.  $n_k$  is therefore a zero-mean, exponentially-correlated random variable whose standard deviation

is  $\sigma$ . The constant  $a_w$  can have a range of values from -1 to +1. For a stable variable,  $a_w$  is restricted to values between 0 and +1. For  $a_w \rightarrow 0$ ,  $n_k$  changes rapidly and tends to be uncorrelated from sample to sample. For  $a_w \rightarrow 1$ , the behaviour of  $n_k$  becomes more sluggish and it tends to change little from sample to sample.

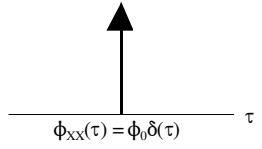
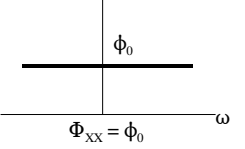
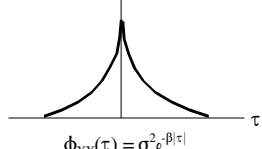
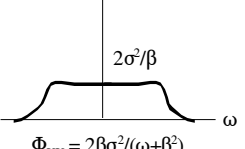
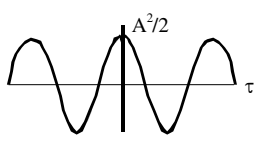
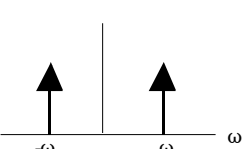
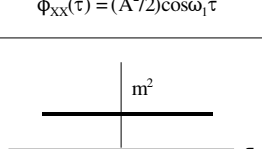
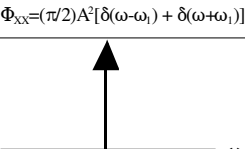
Process	Autocorrelation Function ( $\phi_{xx}$ )	Power Spectral Density ( $\Phi_{xx}$ )
White Noise	 $\phi_{xx}(\tau) = \phi_0 \delta(\tau)$	 $\Phi_{xx} = \phi_0$
Markov Process	 $\phi_{xx}(\tau) = \sigma^2 e^{-\beta \tau }$	 $\Phi_{xx} = 2\beta\sigma^2/(\omega+\beta^2)$
Sinusoid	 $\phi_{xx}(\tau) = (A^2/2)\cos\omega_1\tau$	 $\Phi_{xx} = (\pi/2)A^2[\delta(\omega-\omega_1) + \delta(\omega+\omega_1)]$
Random Bias	 $\phi_{xx}(\tau) = m^2$	 $\Phi_{xx} = 2\pi m^2 \delta(\omega)$

Figure. 4. Description of common random processes (Gelb, 1974).

### 2.3 C-SCPT SEED™ Formulation

The C-SCPT SEED™ algorithm uses real-time Bayesian Recursive Estimation (BRE) digital filtering techniques to analyze the raw SCPT data. Baziw (2002b, 2004b, 2005, 2006, and 2011) outlines in detail the different mathematical tools such as Kalman filtering (KF), particle filter, and Hidden Markov Model filtering (HMM) which are offered in BRE. In general terms, AMS source waves defined as frequency anomalies are identified and extracted within statistically describable (Gauss-Markov) background noise.

As a first step the C-SCPT SEED™ algorithm applies a bank of finite sinusoids ( $i = 1$  to  $N$ ) with dominant frequencies varying from low to high (e.g., 30 Hz to 430 Hz). The seismic event is approximated as an AMS, whereby the sinusoid is modulated by an amplitude modulating term (AMT) as previously described. As illustrated in Figure 5, a fixed set of possible sinusoids with corresponding dominant frequencies is specified at the outset. A bank of Kalman Filters are then utilized, whereby the possible seismic event is approximated as a sinusoid multiplied by an AMT. The KF system equa-

tions include the AMT components which are modeled as a two state first order Taylor series with the velocity component represented by a Gauss-Markov process. The KF measurement equations incorporate the sinusoidal components  $\sin(\omega_i t)$  where  $\omega_i = 2\pi f_i$  and  $f_i$  is the dominant frequency. The frequency components are incorporated as states within a HMM filter formulation. The background noise is also included within the KF system equations through the Gauss-Markov process.

The background noise parameters of variance,  $\sigma^2$ , and time constant,  $T_c$ , are automatically derived from the recorded seismic data by windowing on the noise portion and calculating the auto-correlation. For example, on the initiation of the C-SCPT the data acquisition commences acquiring data at the user specified sampling rate  $\Delta$ . A ring buffer of approximately 9000 points is populated with seismic data. The ring buffer is divided into three time windows (e.g., 3000 points). The variance of each time window is calculated and the window with the lowest variance value is defined to be ambient noise. An auto-correlation is automatically calculated on the ambient noise where the parameters  $\sigma^2$  and  $T_c$  are readily obtained.

The ring buffer of data with parameters  $\sigma^2$  and  $T_c$  is then feed into the C-SCPT SEED™ algorithm for signal processing and event detection. The C-SCPT SEED™ algorithm calculates the AMT component and the dominant frequency of the AMS source if present. The C-SCPT SEED™ algorithm must complete filtering and event detection within  $\Delta \times$  ring buffer size (e.g. 9000 point ring buffer and sampling rate of 5Khz results in a maximum processing time of 1.8 seconds) prior extracting the next set of data from the ring buffer.

When a trigger is initiated (e.g., SH hammer striking steel beam (Campanella et. al. (1986) and Baziw (1993)) the filtered AMT and raw seismic data is stored to file at the user specified sampling rate, sample time and pre-trigger when source impact is made. The real-time arrival time of the source wave (required for relative arrival time estimation and subsequent interval velocity calculation Baziw ((1993 and 2002a)) is defined by applying a second event detection algorithm utilizing a short term average – long term average ratio (STA/LTA) (Baziw (2002b, 2004b and 2005)) technique. The STA/LTA portion of the C-SCPT SEED™ algorithm is applied to the derived AMT to determine the reference arrival time of the source wave. If the user specified threshold was exceeded (“event”) and the estimated frequency resided within a user specified bandwidth (e.g., P-wave and S-wave bandwidth) then the time location of the event is defined to be the arrival time of the source wave.

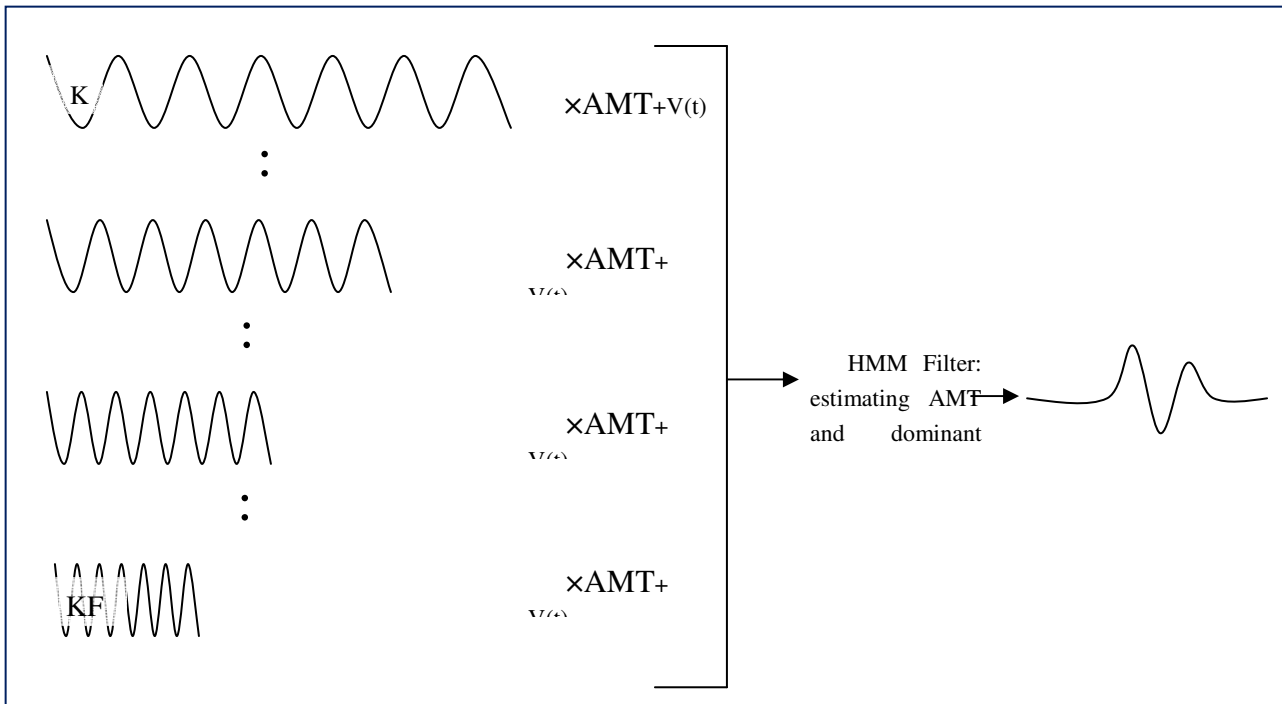


Figure 5. *C-SCPT SEED™* algorithm configuration.

### 3 *C-SCPT SEED™* PERFORMANCE RESULTS

The performance of the *C-SCPT SEED™* algorithm is assessed by considering challenging synthetic data. Figure 6 illustrates a Berlage source wave (Baziw (2005, 2006, and 2011)) with a dominant frequency of 100 Hz, arrival time of 40 ms and maximum absolute amplitude of 7.2.

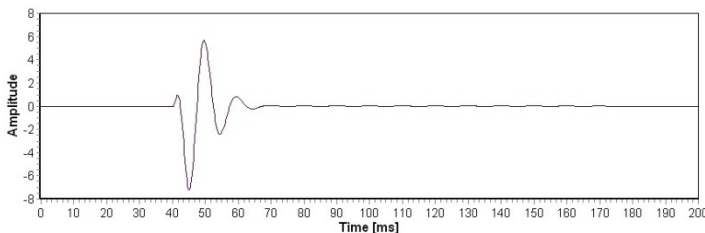


Figure 6. Berlage source wave with dominant frequency of 100 Hz.

#### 3.1 Example 1:

The SC source wave shown in Fig. 6 is embedded within measurement noise with variance  $\sigma^2$  of 6 units<sup>2</sup> and time constant  $T_C$  of 1 ms as illustrated in Fig. 7. The *C-SCPT SEED™* algorithm is then applied on this noisy seismogram with a HMM frequency bandwidth and resolution of 30 - 430 Hz and 2 Hz, respectively. A STA/LTA threshold of 1.2 was specified.

The resulting AMT and STA/LTA is illustrated in Figs. 7(B) and 7(C), respectively. The *C-SCPT SEED™* algorithm also provides the dominant frequencies when the STA/LTA ratio exceeds the threshold of 1.2 as shown in Fig. 7(D).

The results using the using the *C-SCPT SEED™* algorithm can be compared with the outcome when using a standard frequency filtering algorithm (applying an eight order digital bandpass (30 Hz to 150 Hz filter) as illustrated in Fig. 8. It is clear that *C-SCPT SEED™* algorithm provides a considerable SNR improvement compared to the standard frequency filtering.

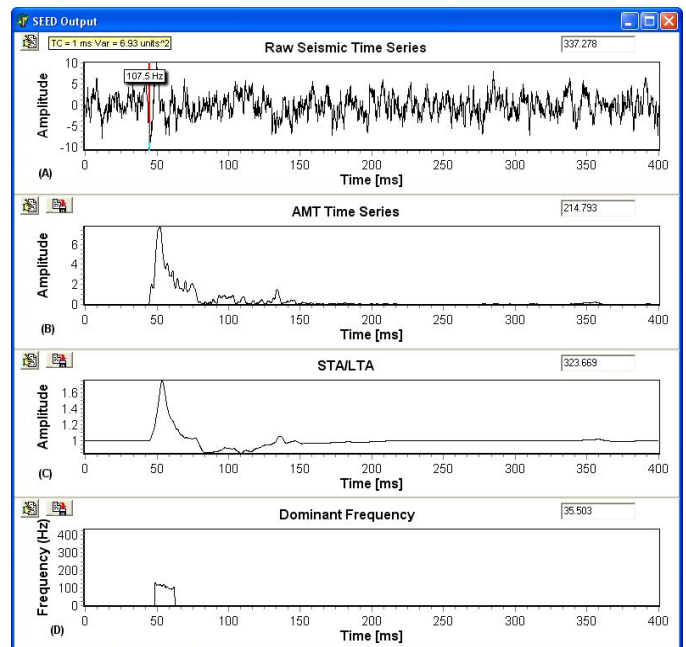


Figure 7.(A) Seismogram with source wave of Figure 6 embedded in measurement noise; (B) Derived AMT using the *C-SCPT SEED™* algorithm; (C) Derived STA/LTA using the *C-SCPT SEED™* algorithm; (D) Estimated frequencies when STA/LTA threshold of 1.2 exceeded using the *C-SCPT SEED™* algorithm.

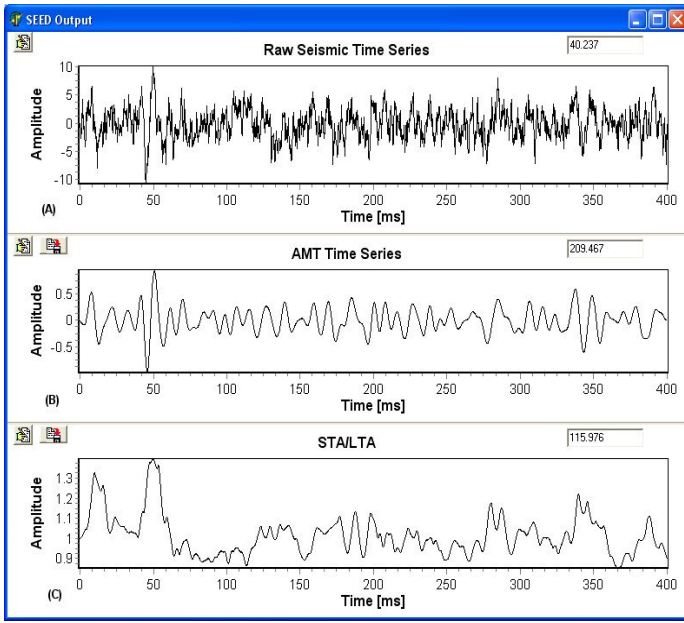


Figure 8. (A) Seismogram with source wave of Figure 6 embedded in measurement noise; (B) Derived AMT after applying an eight-order zero phase bandpass (30 Hz to 150 Hz) filter; (C). Derived STA/LTA of filtered trace.

### 3.2 Example 2 ( $\sigma^2 = 9 \text{ units}^2$ , $T_C = 3 \text{ ms}$ ):

The source wave shown in Figure 6 is embedded within measurement noise with variance of  $9 \text{ units}^2$  and time constant of 3 ms as illustrated in Figure 9(A). The *C-SCPT SEED*<sup>TM</sup> algorithm is then applied on the noisy seismogram of Fig. 9(A) where a HMM frequency bandwidth and resolution of 30 Hz to 430 Hz and 2 Hz is applied. A STA/LTA threshold of 1.2 was specified.

The *C-SCPT SEED*<sup>TM</sup> estimated AMT and STA/LTA is illustrated in Figs. 10(B) and 10(C), respectively. Dominant frequencies are estimated when the STA/LTA ratio exceeds the threshold of 1.2 as shown in Fig. 10(D). Figure 10(A) shows the *C-SCPT SEED*<sup>TM</sup> estimated noise statistics (variance = 6.9 and time constant = 2 ms), the averaged dominant frequency estimate (108.8 Hz (true value = 100 Hz) - averaged over time window where STA/LTA ratio exceeds the threshold of 1.2 as is illustrated in Fig. 10(D)) and arrival time estimate (denoted by vertical red bar).

The impressive *C-SCPT SEED*<sup>TM</sup> results outlined in Fig. 10 are compared with a standard frequency filtering algorithm as illustrated in Fig. 11. Figure 11(B) shows the seismogram of Figs. 10(A) and 11(A) with an eight order digital bandpass (30 Hz to 150 Hz) filter applied. The STA/LTA of Fig. 11(B) is shown in Fig. 11(C). It is clear from comparing Figs. 11(B) and 11(C) with Figs. 10(B) and 11(C) that the *C-SCPT SEED*<sup>TM</sup> algorithm provided considerable S/N improvement and allowed for dominant frequency and noise statistics estimation.

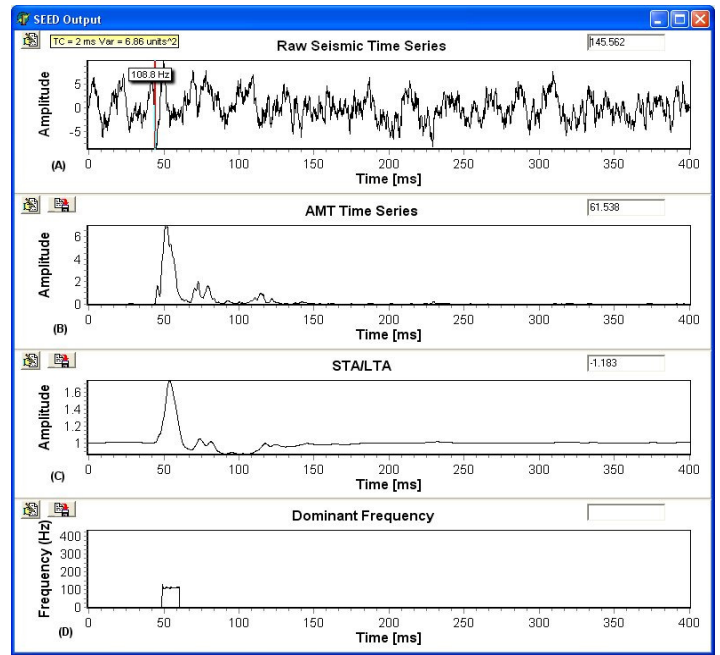


Figure 10. (A) Seismogram with source wave of Figure 6 embedded in measurement noise with *C-SCPT SEED*<sup>TM</sup> estimated arrival time, dominant frequency and ambient noise statistics illustrated. (B) *C-SCPT SEED*<sup>TM</sup> estimated AMT. (C) *C-SCPT SEED*<sup>TM</sup> estimated STA/LTA. (D) *SEED*<sup>TM</sup> estimated frequencies when STA/LTA threshold of 1.2 exceeded.

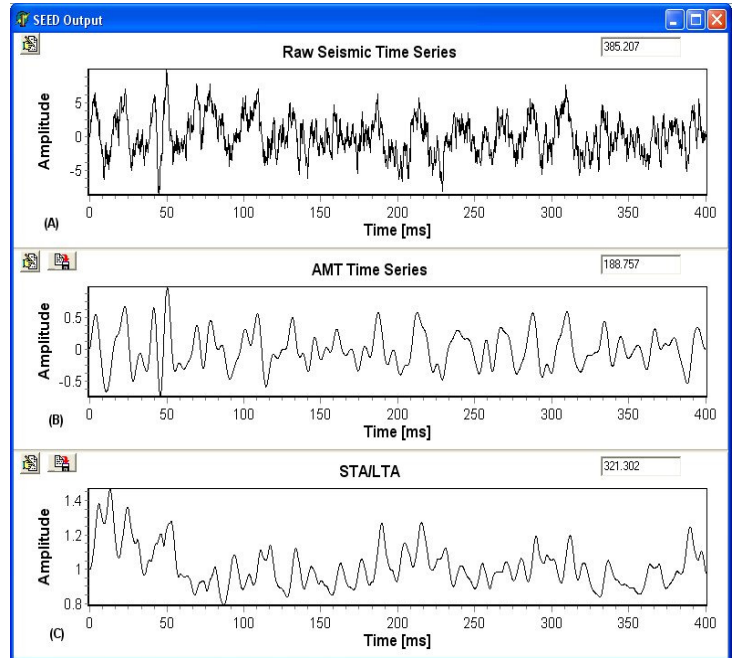


Figure 11. (A) Seismogram with source wave of Figure 6 embedded in ambient noise with variance of  $9 \text{ units}^2$  and time constant of 3 ms. (B) Output after applying an eight-order zero phase bandpass (30 Hz to 150 Hz) to seismogram in (A). STA/LTA of filtered trace in (B).

### 3.3 Example 3 ( $\sigma^2 = 12 \text{ units}^2$ , $T_C = 1 \text{ ms}$ ):

The source wave shown in Figure 6 is embedded within measurement noise with variance of  $12 \text{ units}^2$  and time constant of  $1 \text{ ms}$  as illustrated in Fig. 12(A). The *C-SCPT SEED*<sup>TM</sup> algorithm is then applied on the noisy seismogram of Fig. 12(A) where a HMM frequency bandwidth and resolution of  $30 \text{ Hz}$  to  $430 \text{ Hz}$  and  $2 \text{ Hz}$  is applied, respectively. A STA/LTA threshold of  $1.2$  was specified.

The *C-SCPT SEED*<sup>TM</sup> estimated AMT and STA/LTA is illustrated in Figs. 12(B) and 12(C), respectively. Dominant frequencies are estimated when the STA/LTA ratio exceeds the threshold of  $1.2$  as shown in Fig. 12(D). Figure 12(A) shows the *SEED*<sup>TM</sup> estimated noise statistics (variance =  $11.2$  and time constant =  $1 \text{ ms}$ ), the averaged dominant frequency estimate ( $115 \text{ Hz}$  (true value =  $100 \text{ Hz}$ ) - averaged over time window where STA/LTA ratio exceeds the threshold of  $1.2$  as is illustrated in Fig. 12(D)) and arrival time estimate (denoted by vertical red bar).

The *C-SCPT SEED*<sup>TM</sup> results outlined in Fig. 12 are compared with a standard frequency filtering algorithm as illustrated in Fig. 13. Figure 13(B) shows the seismogram of Figs. 12(A) and 13(A) with an eight order digital bandpass ( $30 \text{ Hz}$  to  $150 \text{ Hz}$ ) filter applied. The STA/LTA of Fig. 13(B) is shown in Fig. 13(C). It is clear from comparing Figs. 13(B) and 13(C) with Figs. 12(B) and 12(C) that the *C-SCPT SEED*<sup>TM</sup> algorithm provided considerable S/N improvement and allowed for dominant frequency and noise statistics estimation.

## 4 CONCLUSIONS

There is considerable interest among *in-situ* engineers to develop continuous seismic cone penetration test (*C-SCPT*) instrumentation, data acquisition hardware and software and signal processing algorithms. This endeavour arises from the fact that there is significant latency when carrying out a standard SCPT investigation due to the requirement of establishing a low noise environment. The pauses and delays in SCPT are namely threefold. 1) The string is unclamped to avoid waves generated by the shear wave source traveling through the CPT rods to the receivers. 2) The engine of the *in-situ* vehicle is turned off to reduce measurements noise. 3) Data stacking is carried by averaging the recorded seismic data from multiple source generations at each depth increment. The most important consideration in *C-SCPT* is obviously the real-time signal enhancement and event detection.

This paper has outlined a new algorithm referred to as the *C-SCPT SEED*<sup>TM</sup> which allows for real-time signal processing and enhancement of *C-SCPT* data and the ability to estimate arrival times. This

would facilitate real-time interval velocity estimation as the probe is advanced within the ground. The *C-SCPT SEED*<sup>TM</sup> algorithm uses real-time Bayesian recursive estimation digital filtering techniques (e.g., Kalman filtering, particle filter, and Hidden Markov Model filtering) to analyze the *C-SCPT* data in real-time. The *C-SCPT SEED*<sup>TM</sup> algorithm models measurement noise in a statistical manner (Gauss-Markov process) where the parameters of variance and time constant are estimated directly from the raw data in real-time. This is in contrast to standard SCPT digital frequency filters where it is assumed that the source wave and measurement noise frequency spectra have distinct separation and the measurement noise is simply described by a set bandwidth of frequency components.

In general terms, In the *C-SCPT SEED*<sup>TM</sup> algorithm source waves defined as frequency anomalies are identified and extracted within statistically describable (Gauss-Markov) background noise. It is shown in this paper that BCE's *C-SCPT SEED*<sup>TM</sup> algorithm provides considerable signal enhancement and event detection advantages when processing *C-SCPT* seismic data, such as: • Ability to identify source wave "events" embedded in high variance and correlated noise environments • Significant S/N improvement • Source wave arrival time estimation • Ability to derive noise statistics • Dominant frequency estimation.

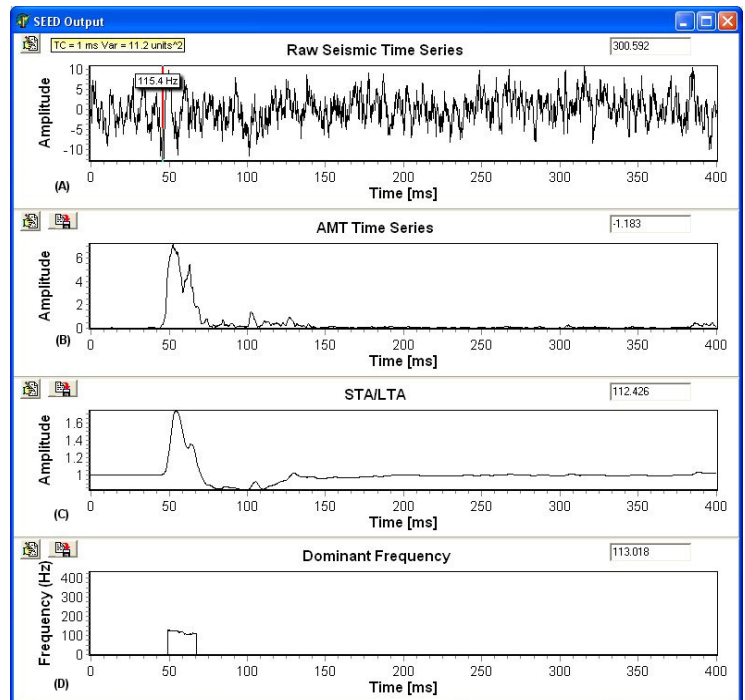


Figure 12. (A) Seismogram with source wave of Figure 6 embedded in ambient noise with *C-SCPT SEED*<sup>TM</sup> estimated arrival time, dominant frequency and ambient noise statistics illustrated. (B) *C-SCPT SEED*<sup>TM</sup> estimated AMT. (C) *SEED*<sup>TM</sup> estimated STA/LTA. (D) *C-SCPT SEED*<sup>TM</sup> estimated frequencies when STA/LTA threshold of  $1.2$  exceeded.

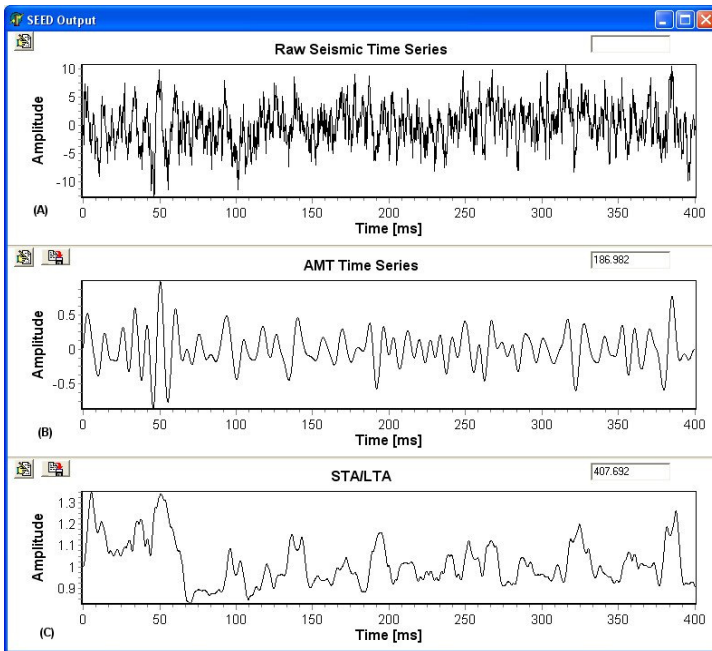


Figure 13. (A) Seismogram with source wave of Figure 6 embedded in ambient noise with variance of 12 units<sup>2</sup> and time constant of 1 ms. (B) Output after applying an eight-order zero phase bandpass (30 Hz to 150 Hz) to seismogram in (A). STA/LTA of filtered trace in (B).

## REFERENCES

- Andrus, R.D., Stokoe, K.H., & Chung, R.M. 1999. Draft guidelines for evaluating liquefaction resistance using shear wave velocity measurements and simplified procedures. NISTIR 6277. National Institute of Standards and Technology, Gaithersburg, Md.
- Finn, W.D.L. 1984. Dynamic response analysis of soils in engineering practice. In *Mechanics of engineering materials*. John Wiley & Sons Ltd., New York. Chapter 13.
- Campanella, R.G., Robertson, FTC and Gillespie, D. 1986. Seismic cone penetration test. Proc. IN SITU86. ASCE, Geot. Spec. Publ. No. 6, June: 116-130.
- ASTM D7400 – 08. 2008. Standard Test Methods for Downhole Seismic Testing.
- Baziw, E. 1993. Digital filtering techniques for interpreting seismic cone data. *Journal of Geotechnical Engineering*, ASCE, 119(6), 98-1018.
- Baziw, E. 2002a. Derivation of seismic cone interval velocities utilizing forward modelling and the downhill simplex method. *Canadian Geotechnical Journal*, 39: 1-12.
- Baziw, E. 2004a. Two and three dimensional imaging utilizing the seismic cone penetrometer. In *Proceedings of the 2nd International Conference on Geotechnical Site Characterization (ISC-2)*, Porto, Portugal, 19-22 Sept. Millpress Science Publishers, 1611-1618.
- Baziw, E. & Weir-Jones, I. 2002b. Application of Kalman filtering techniques for microseismic event detection. *Pure Appl. Geophys.*, vol. 159, pp. 449-473.
- Baziw, E., Nedilko, B., and Weir-Jones, I. 2004b. Microseismic event detection Kalman filter: derivation of the noise covariance matrix and automated first break determination for

accurate source location estimation”, *Pure Appl. Geophys.*, vol. 161, pp. 303-329.

Baziw, E. 2005. Real-Time Seismic Signal Enhancement Utilizing a Hybrid Rao-Blackwellised Particle Filter and Hidden Markov Model Filter”, *IEEE Geosci. Remote Sensing Letters (GRSL)*, vol. 2, no. 4, pp. 418-422.

Baziw, E. and Ulrych, T.J. 2006. Principle phase decomposition – a new concept in blind seismic deconvolution. *IEEE Transactions on Geoscience and Remote Sensing*, vol. 44, no. 8, 2271-2281.

Baziw, E. 2011. Incorporation of Iterative Forward Modeling into the Principle Phase Decomposition Algorithm for Accurate Source Wave and Reflection Series Estimation. vol. 49, No. 2, 1775-1785.

Amini, A. and Howie, J.A. 2005. Numerical simulation of downhole seismic cone signals. *Canadian Geotechnical Journal*, vol. 42(2), pp. 574-586.

Baziw, E., Tichy, J., & de Caprona, G. 2000. Data acquisition in seismic cone penetration testing. In *Proceedings of the 3rd International Symposium on Integrated Technical Approaches to Site Characterization (ITASCE)*, Argonne, IL, pp.69-72. Argonne National Laboratory.

Gelb, A. 1974. *Applied Optimal Estimation* (4th ed.). Cambridge, Mass: MIT Press.